

A Versatile Tripodal Amide Receptor for the Encapsulation of Anions or Hydrated Anions via Formation of Dimeric Capsules

M. Arunachalam and Pradyut Ghosh*

Department of Inorganic Chemistry, Indian Association for the Cultivation of Science, 2A & 2B Raja S. C. Mullick Road, Kolkata 700032, India

Received August 18, 2009

A bowl-shaped tripodal receptor with an appropriately positioned amide functionality on the benzene platform and electron-withdrawing *p*-nitrophenyl terminals (**L**¹) has been designed, synthesized, and studied for the anion binding properties. The single-crystal X-ray crystallographic analysis on crystals of **L**¹ with tetrabutylammonium salts of nitrate (**1**), acetate (**2**), fluoride (**3**), and chloride (**4**) obtained in moist dioxane medium showed encapsulation of two NO₃⁻, [(AcO)₂(H₂O)₄]²⁻, [F₂(H₂O)₆]²⁻, and [Cl₂(H₂O)₄]²⁻ respectively as the anionic guests inside the staggered dimeric capsular assembly of **L**¹. The *p*-nitro substitution in the aryl terminals assisted the formation of dimeric capsular assembly of **L**¹ exclusively upon binding/encapsulating above different guests. Though **L**¹ demonstrates capsule formation upon anion or hydrated anion complexation for all of the anions studied here, its positional isomer with the *o*-nitro-substituted tripodal triamide receptor **L**² selectively formed the dimeric capsular assembly upon encapsulation of [F₂(H₂O)₆]²⁻ and noncapsular aggregates in the cases of other anions such as Cl⁻, NO₃⁻, and AcO⁻. Interestingly, structural investigations upon anion exchange of the complexes revealed that both isomers have selectivity toward the formation of a [F₂(H₂O)₆]²⁻ encapsulated dimeric capsule. In contrast, solution-state ¹H NMR titration studies of **L**¹ and **L**² in DMSO-*d*₆ with AcO⁻ indicated 1:3 (host:guest) binding.

Introduction

In recent years considerable effort has been made in elucidating the coordination chemistry of anions because of their vital roles in biological systems, medicine, catalysis, and environmental issues and the development of new anion

receptors based on organic frameworks continues to attract considerable research effort.¹ Numerous synthetic anion receptors containing polyammonium,² amide,³ urea,⁴ pyrrole,⁵ or indole⁶ groups incorporated in increasingly complicated supramolecular skeletons target the efficiency of natural receptors. Recent studies indicate that the receptor for anions of environmental relevance such as fluoride should target the hydrated ion rather than the naked ion.⁷ This is because in the real world anions mostly exist in hydrated form. Molecular capsules in general, and those obtained by self-assembly in particular, are fascinating molecular systems that have attracted the attention of the scientific community over the past decade.⁸ Self-assembled capsules of bowl-shaped molecules have been studied on several occasions due to their possible applications in molecular storage, drug delivery, sensors, catalysts, or molecular reactors. One of the

*To whom correspondence should be addressed. E-mail: icpg@iacs.res.in.
(1) (a) Bianchi, A.; Bowman-James, K.; García-España, E., Eds. *Supramolecular Chemistry of Anions*; Wiley-VCH: New York, 1997. (b) Sessler, J. L.; Gale, P. A.; Cho, W.-S. *Anion Receptor Chemistry: Monographs in Supramolecular Chemistry*; RSC Publishing: Cambridge, U.K., 2006. (c) Gale, P. A.; García-Garrido, S. E.; Garric, J. *Chem. Soc. Rev.* **2008**, *37*, 151–190. (d) Beer, P. D.; Gale, P. A. *Angew. Chem., Int. Ed.* **2001**, *40*, 486–516. (e) Special Issue: 35 Years of Synthetic Receptor Chemistry: *Coord. Chem. Rev.* **2003**, *240*. (f) Special Issue: Anion Coordination Chemistry II: *Coord. Chem. Rev.* **2006**, *250*.
(2) (a) Bowman-James, K. *Acc. Chem. Res.* **2005**, *38*, 671–678. (b) Lakshminarayanan, P. S.; Kumar, D. K.; Ghosh, P. *Inorg. Chem.* **2005**, *44*, 7540–7546. (c) Lakshminarayanan, P. S.; Suresh, E.; Ghosh, P. *Angew. Chem., Int. Ed.* **2006**, *45*, 3807–3811. (d) Arunachalam, M.; Ravikumar, I.; Ghosh, P. *J. Org. Chem.* **2008**, *73*, 9144–9147. (e) Arunachalam, M.; Suresh, E.; Ghosh, P. *Tetrahedron* **2007**, *63*, 11371–11376. (f) Mason, S.; Clifford, T.; Seib, L.; Kuczera, K.; Bowman-James, K. *J. Am. Chem. Soc.* **1998**, *120*, 8899–8900.
(3) (a) Kang, S. O.; Powell, D.; Day, V. W.; Bowman-James, K. *Angew. Chem., Int. Ed.* **2006**, *45*, 1921–1925. (b) Kang, S. O.; Begum, R. A.; Bowman-James, K. *Angew. Chem., Int. Ed.* **2006**, *45*, 7882–7894. (c) Bisson, A. P.; Lynch, V. M.; Monahan, M.-K. C.; Anslyn, E. V. *Angew. Chem., Int. Ed.* **1997**, *36*, 2340–2342.
(4) (a) Brooks, V. S. J.; García-Garrido, S. E.; Light, M. E.; Cole, P. A.; Gale, P. A. *Chem. Eur. J.* **2007**, *13*, 3320–3329. (b) García-Garrido, S. E.; Caltagirone, C.; Light, M. E.; Gale, P. A. *Chem. Commun.* **2007**, 1450–1452. (c) Turner, D. R.; Paterson, M. J.; Steed, J. W. *Chem. Commun.* **2008**, 1395–1397.

(5) (a) Sessler, J. L.; Camiolo, S.; Gale, P. A. *Coord. Chem. Rev.* **2003**, *240*, 17–55. (b) Sessler, J. L.; Kim, S. K.; Gross, D. E.; Lee, C.-H.; Kim, J. S.; Lynch, V. M. *J. Am. Chem. Soc.* **2008**, *130*, 13162–13166.
(6) (a) Gale, P. A. *Chem. Commun.* **2008**, 4525–4540. (b) Caltagirone, C.; Gale, P. A.; Hiscock, J. R.; Brooks, S. J.; Hursthouse, M. B.; Light, M. E. *Chem. Commun.* **2008**, 3007–3009. (c) Caltagirone, C.; Hiscock, J. R.; Hursthouse, M. B.; Light, M. E.; Gale, P. A. *Chem. Eur. J.* **2008**, *14*, 10236–10243. (d) Sessler, J. L.; Cho, D. G.; Lynch, V. J. *Am. Chem. Soc.* **2006**, *128*, 16518–16519. (e) Chang, K.-J.; Moon, D.; Lah, M. S.; Jeong, K.-S. *Angew. Chem., Int. Ed.* **2005**, *44*, 7926–7929.
(7) (a) Cametti, M.; Rissanen, K. *Chem. Commun.* **2009**, 2809–2829. (b) Arunachalam, M.; Ghosh, P. *Chem. Commun.* **2009**, 5389–5391.

most fascinating features of molecular capsules is their ability to isolate the encapsulated guests from the bulk. Self-complementary units of a molecular capsule are generally based

(8) (a) Varner, J. E., Ed. *Self-Assembling Architecture*; Wiley-Liss: New York, 1988. (b) Lehn, J.-M. *Supramolecular Chemistry, Concepts and Perspectives*; VCH: Weinheim, Germany, 1995. (c) Cram, D. J. *Nature* **1992**, *356*, 29–36. (d) Chapman, R. G.; Sherman, J. C. *Tetrahedron* **1997**, *53*, 15911–15945. (e) Jasat, A.; Sherman, J. C. *Chem. Rev.* **1999**, *99*, 931–967. (f) Conn, M. M.; Rebek, J., Jr. *Chem. Rev.* **1997**, *97*, 1647–1668. (g) Fujita, M.; Umemoto, K.; Yoshizawa, M.; Fujita, N.; Kusukawa, T.; Biradha, K. *Chem. Commun.* **2001**, 509–518. (h) Hof, F.; Craig, S. L.; Nuckolls, C.; Rebek, J., Jr. *Angew. Chem., Int. Ed.* **2002**, *41*, 1488–1508. (i) Shimizu, K. D.; Rebek, J., Jr. *Proc. Natl. Acad. Sci. U.S.A.* **1995**, *92*, 12403–12407. (j) Böhmer, V.; Mogck, O.; Pons, M.; Paulus, E. F. In *NMR in Supramolecular Chemistry*; Pons, M., Ed.; Kluwer Academic: Dordrecht, The Netherlands, 1999; pp 45–60. (k) Rebek, J., Jr. *Acc. Chem. Res.* **1999**, *32*, 278–286.

(9) (a) Kerckhoffs, J. M. C. A.; Cate, M. G. J. T.; Mateos-Timoneda, M. A.; Leeuwen, F. W. B. V.; Snellink-Ruël, B.; Spek, A. L.; Kooijman, H.; Calama, M. C.; Reinhoudt, D. N. *J. Am. Chem. Soc.* **2005**, *127*, 12697–12708. (b) Rebek, J., Jr. *Chem. Commun.* **2000**, 637–643.

(10) (a) MacGillivray, L. R.; Atwood, J. L. *Nature* **1997**, *389*, 469–472. (b) Kobayashi, K.; Shirasaka, T.; Horn, E.; Furukawa, N.; Yamaguchi, K.; Sakamoto, S. *Chem. Commun.* **2000**, 41–42. (c) Ajami, D.; Rebek, J., Jr. *Angew. Chem., Int. Ed.* **2007**, *46*, 9283–9286. (d) Heinz, T.; Rudkevich, D. M.; Rebek, J., Jr. *Nature* **1998**, *394*, 764–766. (e) Rose, K. N.; Barbour, L. J.; Orr, G. W.; Atwood, J. L. *Chem. Commun.* **1998**, 407–408. (f) Shivanyuk, A.; Saadioui, M.; Broda, F.; Thondorf, I.; Vysotsky, M. O.; Rissanen, K.; Kolehmainen, E.; Böhmer, V. *Chem. Eur. J.* **2004**, *10*, 2138–2148. (g) Mansikkamäki, H.; Nissinen, M.; Rissanen, K. *Chem. Commun.* **2002**, 1902–1903.

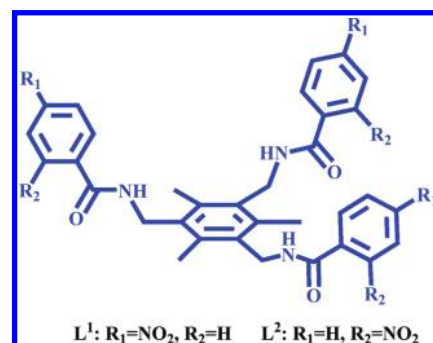
(11) (a) Wylter, R.; de Mendoza, J.; Rebek, J., Jr. *Angew. Chem., Int. Ed.* **1993**, *32*, 1699–1701. (b) Szabo, T.; O'Leary, B. M.; Rebek, J., Jr. *Angew. Chem., Int. Ed.* **1998**, *37*, 3410–3413. (c) Meissner, R. S.; Rebek, J., Jr.; de Mendoza, J. *Science* **1995**, *270*, 1485–1488. (d) Grotzfeld, R. M.; Branda, N.; Rebek, J., Jr. *Science* **1996**, *271*, 487–489. (e) Elemans, J. A. A. W.; Rowan, A. E.; Nolte, R. J. M. *Ind. Eng. Chem. Res.* **2000**, *39*, 3419–3428.

(12) (a) Rudzevich, Y.; Rudzevich, V.; Schollmeyer, D.; Thondorf, I.; Böhmer, V. *Org. Lett.* **2005**, *7*, 613–616. (b) Bray, D. J.; Antonoli, B.; Clegg, J. K.; Gloe, K.; Gloe, K.; Jolliffe, K. A.; Lindoy, L. F.; Weic, G.; Wenzel, M. *Dalton Trans.* **2008**, 1683–1685. (c) L-Lázaro, A.; Pastor, A.; Prince, P. D.; Steed, J. W.; Arakawa, R. *Chem. Commun.* **2001**, 169–170. (d) Alajarm, M.; Pastor, A.; Orenes, R.-A.; Steed, J. W. *J. Org. Chem.* **2002**, *67*, 7091–7095. (e) Alajarm, M.; Pastor, A.; Orenes, R.-A.; Steed, J. W.; Arakawa, R. *Chem. Eur. J.* **2004**, *10*, 1383–1397. (f) Alajarm, M.; Pastor, A.; Orenes, R.-A.; Viviente, E. M.; Rüegger, H.; Pregosin, P. S. *Chem. Eur. J.* **2007**, *13*, 1559–1569. (g) Alajarm, M.; Pastor, A.; Orenes, R.-A.; Martínez-Viviente, E.; Pregosin, P. S. *Chem. Eur. J.* **2006**, *12*, 877–886. (h) Alajarm, M.; Pastor, A.; Orenes, R.-A.; Goeta, A. E.; Steed, J. W. *Chem. Commun.* **2008**, 3992–3994. (i) Rudzevich, Y.; Rudzevich, V.; Schollmeyer, D.; Thondorf, I.; Böhmer, V. *Org. Biomol. Chem.* **2006**, *4*, 3938–3944. (j) Bray, D. J.; Liao, L.-L.; Antonoli, B.; Gloe, K.; Lindoy, L. F.; McMurtrie, J. C.; Wei, G.; Zhang, X.-Y. *Dalton Trans.* **2005**, 2082–2083.

(13) (a) Nativi, C.; Cacciarini, M.; Francesconi, O.; Vacca, A.; Moneti, G.; Lenco, A.; Roelens, S. *J. Am. Chem. Soc.* **2007**, *129*, 4377–4385. (b) Wallace, K. J.; Belcher, W. C.; Turner, D. R.; Syed, K. F.; Steed, J. W. *J. Am. Chem. Soc.* **2003**, *125*, 9699–9715. (c) Zyryanov, G. V.; Palacios, M. A.; Anzenbacher, P. *Angew. Chem., Int. Ed.* **2007**, *46*, 7849–7852. (d) Amendola, V.; Boiocchi, M.; Colasson, B.; Fabbri, L.; Douton, M.-J. R.; Ugozzoli, F. *Angew. Chem., Int. Ed.* **2006**, *45*, 6920–6924. (e) Hennrich, G.; Anslin, E. V. *Chem. Eur. J.* **2002**, *8*, 2218–2224. (f) Arunachalam, M.; Suresh, E.; Ghosh, P. *Tetrahedron Lett.* **2007**, *48*, 2909–2913. (g) Grawe, T.; Schrader, T.; Gurrath, M.; Kraft, A.; Osterod, F. *Org. Lett.* **2005**, *2*, 29–32. (h) Grawe, T.; Schrader, T.; Gurrath, M.; Kraft, A.; Osterod, F. *J. Phys. Org. Chem.* **2000**, *13*, 670–673. (i) Grawe, T.; Schrader, T.; Zadnadar, R.; Kraft, A. *J. Org. Chem.* **2002**, *67*, 3755–3763. (j) Vacca, A.; Nativi, C.; Cacciarini, M.; Pergoli, R.; Roelens, S. *J. Am. Chem. Soc.* **2004**, *126*, 16456–16465.

(14) (a) Zhu, S. S.; Staats, H.; Brandhorst, K.; Grunenberg, J.; Gruppi, F.; Dalcanele, E.; Lützen, A.; Rissanen, K.; Schalley, C. A. *Angew. Chem., Int. Ed.* **2008**, *47*, 788–792. (b) Lankshear, M. D.; Beer, P. D. *Acc. Chem. Res.* **2007**, *40*, 657–668. (c) Gimeno, N.; Vilar, R. *Coord. Chem. Rev.* **2006**, *250*, 3161–3189. (d) Diaz, P.; Mingos, D. M. P.; Vilar, R.; White, A. J. P.; Williams, D. J. *Inorg. Chem.* **2004**, *43*, 7597–7604. (e) Vilar, R. *Angew. Chem., Int. Ed.* **2003**, *42*, 1460–1477. (f) Rais, D.; Yau, J.; Mingos, D. M. P.; Vilar, R.; White, A. J. P.; Williams, D. J. *Angew. Chem., Int. Ed.* **2001**, *40*, 3464–3467. (g) Vilar, R.; Mingos, D. M. P.; White, A. J. P.; Williams, D. J. *Angew. Chem., Int. Ed.* **1998**, *37*, 1258–1261. (h) Fleming, J. S.; Mann, K. L. V.; Carraz, C.-A.; Psillakis, E.; Jeffery, J. C.; McCleverty, J. A.; Ward, M. D. *Angew. Chem., Int. Ed.* **1998**, *37*, 1279–1281.

Chart 1



on conformationally restricted systems such as calixarenes,⁹ resorcinarenes,¹⁰ glycoluril,¹¹ and tripodal¹² derivatives. Among the tripodal systems the 1,3,5-trialkylbenzene core provides some degree of preorganization into a conical conformation with all three binding arms projected in one direction.¹³

Recently anions have been explored in the area of supramolecular assemblies/syntheses in the literature.¹⁴ Our recent studies on 1,3,5-trialkylbenzene-based tripodal receptors functionalized with benzimidazole units showed anion-assisted capsular assembly and disassembly processes¹⁵ and selective encapsulation of hydrated fluoride in a capsular assembly by the tripodal amide receptor **L**² (Chart 1), whereas noncapsular aggregation took place with other anions such as Cl⁻, NO₃⁻, and AcO⁻.^{7b} Herein, we demonstrate that the *p*-nitrobenzoyl-substituted tripodal amide receptor **L**¹ (Chart 1) is a versatile host for encapsulation of two nitrate ions or hydrated forms of acetate, fluoride, and chloride through capsular assembly.

Experimental Section

Materials. All reagents, tetrabutylammonium salts, and solvents for syntheses were purchased from commercial sources and used as received. 1,3,5-Tris(aminomethyl)-2,4,6-trimethylbenzene was prepared as per the modified literature procedure,^{13j} where 1,3,5-tris(bromomethyl)-2,4,6-trimethylbenzene is used instead of 1,3,5-tris(bromomethyl)-2,4,6-triethylbenzene. **L**² was synthesized by following our earlier report.^{7b}

Instrumentation. ¹H NMR spectra were recorded with 300 MHz Bruker DPX-300 and 500 MHz Bruker DPX-500 NMR spectrometers. ¹³C NMR spectra were obtained at 75.47 and 125.77 MHz. ¹⁹F NMR spectra were obtained on a 500 MHz Bruker DPX-500 NMR spectrometer. HRMS experiments were carried out on a Waters QtoF Model YA 263 mass spectrometer in positive ESI mode. Elemental analyses for the synthesized ligand and complexes were carried out with a Perkin-Elmer 2500 series II elemental analyzer. Crystals of the complexes **1–4** were washed with a minimum amount of acetonitrile followed by diethyl ether, and the residue was dried at 75 °C in the oven for 48 h before submitting the samples for elemental analysis.

Ligand Design and Synthesis. For a receptor to bind with the anionic guests, it should possess preorganized anion binding elements decorated on the suitable platform/framework. The designing principles of receptors **L**¹ and **L**² are (i) selection of a suitable rigid platform, (ii) functionalization of the 1,3,5-trimethylbenzene platform with an amide functionality to generate a triamide cleft, and (iii) proper choice of aryl terminals to enhance the binding ability of the receptor toward the anionic

guest(s). It has been well established that the electron-withdrawing substituents on the benzene ring assist the active participation of the aryl $-\text{CH}$ protons toward anion binding via $\text{C}-\text{H}\cdots\text{anion}$ interactions.¹⁶ Considering the above points, we have designed and synthesized tripodal amide receptors on the benzene platform, L^1 and L^2 , having nitro-substituted aryl terminals for anion binding studies.

Synthesis of L^1 . 1,3,5-Tris(aminomethyl)-2,4,6-trimethylbenzene (0.414 g, 2 mmol) and 0.8 mL of triethylamine was dissolved in 100 mL of chloroform, and the mixture was stirred at 0 °C in an ice bath for 25 min under a nitrogen atmosphere. 4-Nitrobenzoyl chloride (1.12 g, 6 mmol, 3 equiv) was added under a nitrogen atmosphere with constant stirring. The formation of a white precipitate in the reaction mixture was observed immediately. The reaction mixture was gradually brought to room temperature and was stirred for 24 h. The precipitate was filtered, and the residue was washed with plenty of water to remove triethylammonium chloride. Then the residue was washed with diethyl ether and dried in air to give 1.05 g of an off-white powder of L^1 . Yield: 81%. ¹H NMR (300 MHz, DMSO-*d*₆; δ (ppm)): 2.42 (s, 9H, $-\text{CH}_3$), 4.57 (d, 6H, $-\text{CH}_2$, $J = 4.4$ Hz), 8.04 (d, 6H, $-\text{CHAr}$, $J = 8.75$ Hz), 8.26 (d, 6H, $-\text{CHAr}$, $J = 8.74$ Hz), 8.77 (t, 3H, $-\text{NH}$, $J = 4.13$ Hz); ¹³C NMR (75 MHz, DMSO-*d*₆; δ (ppm)): 16.59, 123.79, 129.43, 132.82, 137.61, 140.54, 149.36, 165.13. HRMS (ESI): *m/z* 677.4435 [$\text{L} + \text{Na}$]⁺, 693.4414 [$\text{L} + \text{K}$]⁺. Anal. Calcd for $\text{C}_{33}\text{H}_{30}\text{N}_6\text{O}_9$: C, 60.55; H, 4.62; N, 12.84. Found: C, 60.13; H, 4.53; N, 12.93.

Syntheses of Complexes 1–4. Preparation of $\text{L}^1 \cdot \text{TBA} \cdot \text{NO}_3 \cdot (\text{dioxane})$ (1). Complex 1 was prepared by charging an excess (15 equiv) of tetrabutylammonium nitrate into a suspension of L^1 (65 mg, 0.1 mmol) in 15 mL of dioxane. After addition of tetrabutylammonium nitrate the suspension turned clear and the solution was warmed to ~80 °C; then the solution was filtered and allowed to slowly evaporate at room temperature. After 4–5 days colorless crystals of 1 were obtained. Yield: 33%. ¹H NMR (500 MHz, DMSO-*d*₆; δ (ppm)): 0.84 (t, $J = 7.5$ Hz, 12H, $-\text{NCH}_2\text{CH}_2\text{CH}_2\text{CH}_3$), 1.22 (q, $J = 7.3$ Hz, 8H, $-\text{NCH}_2\text{CH}_2\text{CH}_2\text{CH}_3$), 1.49 (m, 8H, $-\text{NCH}_2\text{CH}_2\text{CH}_2\text{CH}_3$), 2.35 (s, 9H, $-\text{CH}_3$), 3.09 (t, 8H, $-\text{NCH}_2\text{CH}_2\text{CH}_2\text{CH}_3$), 4.50 (d, 6H, $J = 4.0$ Hz), 7.98 (d, 6H, $-\text{CHAr}$, $J = 8.5$ Hz), 8.17 (t, 6H, $-\text{CHAr}$, $J = 8.5$ Hz), 8.7 (3H, $-\text{NH}$). ¹³C NMR (125.77 MHz, DMSO-*d*₆; δ (ppm)): 13.96, 16.61, 19.73, 23.61, 58.13, 123.82, 129.49, 132.84, 140.63, 149.42, 165.18. Anal. Calcd for $\text{C}_{49}\text{H}_{66}\text{N}_8\text{O}_{12}$: C, 61.36; H, 6.94; N, 11.68. Found: C, 61.58; H, 7.05; N, 11.74.

Preparation of $\text{L}^1 \cdot \text{TBA} \cdot \text{AcO} \cdot 4\text{H}_2\text{O}$ (2). Complex 2 was prepared by charging an excess (10 equiv) of tetrabutylammonium acetate into the suspension of L^1 (65 mg, 0.1 mmol) in 15 mL of dioxane. After addition of tetrabutylammonium acetate the suspension turned clear and the solution was warmed to ~80 °C; then solution was filtered and allowed to slowly evaporate at room temperature. After 4–5 days colorless crystals of 2 were obtained. Yield: 19%. ¹H NMR (300 MHz, DMSO-*d*₆; δ (ppm)): 0.93 (12H, $-\text{NCH}_2\text{CH}_2\text{CH}_2\text{CH}_3$), 1.30 (8H, $-\text{NCH}_2\text{CH}_2\text{CH}_2\text{CH}_3$), 1.55 (b, 11H, $-\text{NCH}_2\text{CH}_2\text{CH}_2\text{CH}_3$ and $\text{CH}_3\text{COO}-$), 2.41 (s, 9H, $-\text{CH}_3$), 3.17 (t, 8H, $-\text{NCH}_2\text{CH}_2\text{CH}_2\text{CH}_3$), 4.59 (s, 6H, $-\text{NHCH}_2$), 8.13 (d, 6H, $-\text{CHAr}$, $J = 8.7$ Hz), 8.25 (d, 6H, $-\text{CHAr}$, $J = 8.4$ Hz), 9.08 (b, $-\text{NH}$). ¹³C NMR (75 MHz, CDCl_3 ; δ (ppm)): 13.69, 16.38, 19.84, 24.03, 24.55, 40.53, 59.13, 123.31, 129.49, 131.71, 137.78, 140.29, 149.20, 165.74, 147.54, 165.84, 173.67. Anal. Calcd for $\text{C}_{51}\text{H}_{69}\text{N}_7\text{O}_{11}$: C, 64.06; H, 7.27; N, 10.25. Found: C, 64.27; H, 7.33; N, 10.36.

Preparation of $\text{L}^1 \cdot \text{TBA} \cdot \text{F} \cdot 3\text{H}_2\text{O} \cdot 2(\text{dioxane})$ (3). Complex 3 was prepared by charging an excess (10 equiv) of tetrabutylammonium

fluoride into the suspension of L^1 (65 mg, 0.1 mmol) in 15 mL of dioxane. After addition of tetrabutylammonium fluoride the suspension turned clear and the solution was warmed to ~80 °C; then the solution was filtered and allowed to slowly evaporate at room temperature. After 5 days colorless crystals of 3 were obtained. Yield: 28%. ¹H NMR (300 MHz, DMSO-*d*₆; δ (ppm)): 0.95 (t, $J = 6.5$ Hz, 12H, $-\text{NCH}_2\text{CH}_2\text{CH}_2\text{CH}_3$), 1.30 (8H, $-\text{NCH}_2\text{CH}_2\text{CH}_2\text{CH}_3$), 1.57 (8H, $-\text{NCH}_2\text{CH}_2\text{CH}_2\text{CH}_3$), 2.42 (s, 9H, $-\text{CH}_3$), 3.17 (t, 8H, $-\text{NCH}_2\text{CH}_2\text{CH}_2\text{CH}_3$), 4.56 (s, 6H, $-\text{NHCH}_2$), 8.09 (d, 6H, $-\text{CHAr}$, $J = 8.7$ Hz), 8.25 (d, 6H, $-\text{CHAr}$, $J = 8.4$ Hz). ¹³C NMR (75 MHz, DMSO-*d*₆; δ (ppm)): 13.94, 16.51, 19.67, 23.52, 57.98, 123.40, 129.75, 132.95, 136.92, 141.60, 148.90, 164.90. Anal. Calcd for $\text{C}_{49}\text{H}_{66}\text{FN}_7\text{O}_9$: C, 64.24; H, 7.26; N, 10.70. Found: C, 64.03; H, 7.30; N, 10.45.

Preparation of $\text{L}^1 \cdot \text{TBA} \cdot \text{Cl} \cdot 2\text{H}_2\text{O} \cdot 2(\text{dioxane})$ (4). Complex 4 was prepared by charging an excess (10 equiv) of tetrabutylammonium chloride into the suspension of L^1 (65 mg, 100 mmol) in 15 mL of dioxane. After addition of tetrabutylammonium chloride the suspension turned clear and the solution was warmed to ~80 °C; then the solution was filtered and allowed to slowly evaporate at room temperature. After 3–4 days colorless crystals of 4 were obtained. Yield: 36%. ¹H NMR (300 MHz, DMSO-*d*₆; δ (ppm)): 0.91 (t, $J = 7.0$ Hz, 12H, $-\text{NCH}_2\text{CH}_2\text{CH}_2\text{CH}_3$), 1.32 (m, 8H, $-\text{NCH}_2\text{CH}_2\text{CH}_2\text{CH}_3$), 1.55 (m, 8H, $-\text{NCH}_2\text{CH}_2\text{CH}_2\text{CH}_3$), 2.43 (s, 9H, $-\text{CH}_3$), 3.15 (t, 8H, $-\text{NCH}_2\text{CH}_2\text{CH}_2\text{CH}_3$), 4.58 (s, 6H, $-\text{CH}_2$), 8.05 (d, 6H, $-\text{CHAr}$, $J = 8.3$ Hz), 8.26 (d, 6H, $-\text{CHAr}$, $J = 8.2$ Hz), 8.79 (t, $-\text{NH}$). ¹³C NMR (75 MHz, DMSO-*d*₆; δ (ppm)): 13.93, 16.58, 19.64, 23.51, 58.0, 123.81, 129.44, 132.74, 137.58, 140.50, 149.35, 165.23. Anal. Calcd for $\text{C}_{49}\text{H}_{66}\text{ClN}_7\text{O}_9$: C, 63.11; H, 7.13; N, 10.51. Found: C, 62.97; H, 7.18; N, 10.65.

X-ray Crystallographic Analysis. The crystallographic data and details of data collection for 1–4 are given in Table 1. In each case, a crystal of suitable size was selected from the mother liquor, immersed in Paratone oil, and then mounted on the tip of a glass fiber and cemented using epoxy resin. Intensity data for all four crystals were collected using Mo $\text{K}\alpha$ ($\lambda = 0.7107 \text{ \AA}$) radiation on a Bruker SMART APEX diffractometer equipped with a CCD area detector at 100 K. The data integration and reduction were processed with SAINT^{17a} software. An empirical absorption correction was applied to the collected reflections with SADABS.^{17b} The structures were solved by direct methods using SHELXTL¹⁸ and were refined on F^2 by the full-matrix least-squares technique using the SHELXL-97¹⁹ program package. Graphics were generated using PLATON²⁰ and MERCURY 1.3.²¹ In all cases, non-hydrogen atoms were treated anisotropically except for disordered atoms (treated isotropically). All the hydrogen atoms attached to carbon atoms were geometrically fixed. Wherever possible, the amide hydrogen atoms were located from the Fourier map. One of the lattice dioxane molecules was disordered in complex 1. The occupancy factors of these atoms were refined using the FVAR command of the SHELXTL program and isotropically refined. Similarly, one of the arms of L^1 in complex 3 was disordered in two positions. The occupancy factors of these atoms were refined using the FVAR command of the SHELXTL program and isotropically refined. The water molecules encapsulated in complex 2–4 were disordered in two positions, and their occupancy

(17) (a) SAINT and XPREP, version 5.1; Siemens Industrial Automation Inc., Madison, WI, 1995. (b) Sheldrick, G. M. SADABS, Empirical Absorption Correction Program; University of Göttingen, Göttingen, Germany, 1997.

(18) Sheldrick, G. M. SHELXTL Reference Manual, Version 5.1; Bruker AXS: Madison, WI, 1997.

(19) Sheldrick, G. M. SHELXL-97: Program for Crystal Structure Refinement; University of Göttingen, Göttingen, Germany, 1997.

(20) Spek, A. L. PLATON-97; University of Utrecht, Utrecht, The Netherlands, 1997.

(21) Mercury 1.3, supplied with Cambridge Structural Database; CCDC, Cambridge, U.K., 2003–2004.

(16) (a) Berryman, O. B.; Sather, A. C.; Hay, B. P.; Meisner, J. S.; Johnson, D. W. *J. Am. Chem. Soc.* **2008**, *130*, 10895–10897. (b) Bryantsev, V. S.; Hay, B. P. *Org. Lett.* **2005**, *7*, 5031–5034.

Table 1. Crystallographic Parameters of Complexes 1–4

param	1	2	3	4
empirical formula	C ₁₀₆ H ₁₄₈ N ₁₆ O ₂₈	C ₅₁ H ₇₇ N ₇ O ₁₅	C ₅₇ H ₈₈ FN ₇ O ₁₆	C ₅₇ H ₈₆ ClN ₇ O ₁₅
formula wt	2094.40	1028.20	1146.34	1144.78
cryst syst	triclinic	triclinic	triclinic	triclinic
space group	$P\bar{1}$	$P\bar{1}$	$P\bar{1}$	$P\bar{1}$
<i>a</i> (Å)	13.6878(8)	12.484(4)	13.0150(11)	13.0744(6)
<i>b</i> (Å)	15.7779(9)	13.781(4)	13.5935(11)	13.6103(6)
<i>c</i> (Å)	26.9291(17)	16.753(6)	17.5401(15)	17.4610(8)
α (deg)	77.812(2)	85.776(19)	73.679(2)	72.9510(10)
β (deg)	86.317(2)	73.550(18)	83.907(2)	82.7580(10)
γ (deg)	69.6960(10)	72.30(2)	89.519(2)	88.2310(10)
<i>V</i> (Å ³)	5331.2(6)	2633.0(15)	2960.6(4)	2946.8(2)
<i>Z</i>	2	2	2	2
<i>d</i> _{calcd} (g/cm ³)	1.305	1.297	1.286	1.290
cryst size (mm ³)	0.60 × 0.36 × 0.26	0.18 × 0.14 × 0.1	0.24 × 0.16 × 0.14	0.28 × 0.16 × 0.15
diffractometer	Smart CCD	Smart CCD	Smart CCD	Smart CCD
<i>F</i> (000)	2240	1104	1232	1228
μ (Mo K α) (mm ⁻¹)	0.095	0.096	0.096	0.137
<i>T</i> (K)	100 (2)	100 (2)	100 (2)	100 (2)
2 θ _{max} (deg)	25.25	19.99	23.33	21.93
no. of obsd rflns	19 487	4846	8557	7169
no. of params refined	1353	639	747	724
R1; wR2	0.0637; 0.1721	0.0989; 0.2734	0.0558; 0.1552	0.0862; 0.2332
GOF (<i>F</i> ²)	1.052	1.085	0.985	1.048

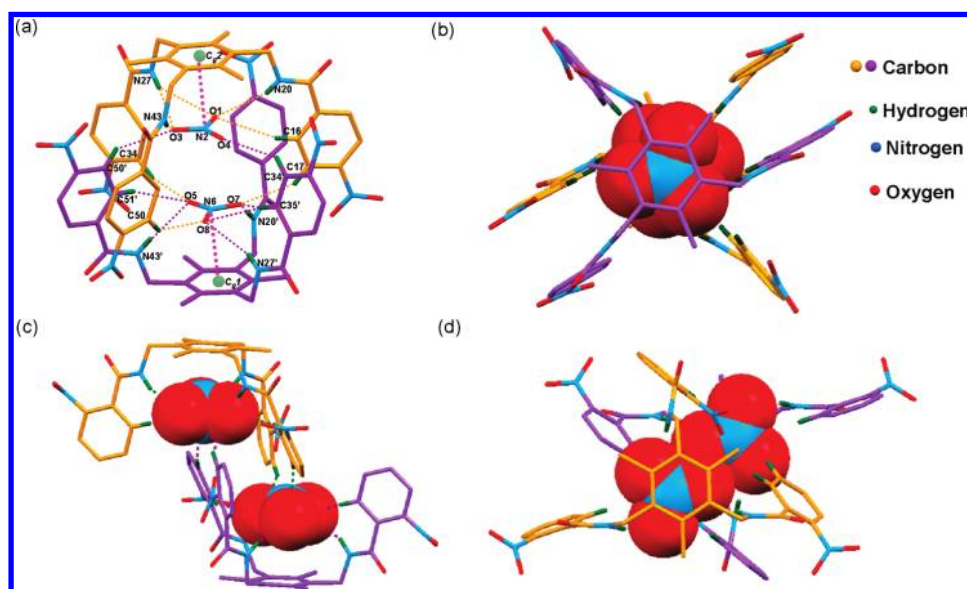


Figure 1. (a) View showing the encapsulated nitrate inside the dimeric capsule and the hydrogen-bonding interactions of nitrate anions with the L^1 receptor molecules in **1**. (b) View along the apical benzene cap showing the encapsulated nitrates inside the staggered dimeric capsular assembly in **1**. (c) Zipperlike assembly of the nitrate complex of L^2 . (d) View along the apical benzene cap showing the encapsulated nitrates inside the noncapsular zipperlike assembly in the nitrate complex of L^2 . Tetrabutylammonium cations, nonbonding hydrogen atoms, and the lattice solvent molecules have been omitted for clarity.

factors were refined using the FVAR command of the SHELXTL program and isotropically refined.

NMR Studies. Solution-state ¹H NMR (300 MHz Bruker) experiments of L^1 with $[n\text{-Bu}]_4\text{N}^+\text{A}^-$ ($\text{A}^- = \text{F}^-, \text{Cl}^-, \text{AcO}^-, \text{NO}_3^-$) were carried out in DMSO-*d*₆ at 25 °C. ¹H NMR titration experiments were performed for L^1 with TBA-AcO in DMSO-*d*₆ at 25 °C. The initial concentration of L^1 was 15.3 mM. Aliquots of anions were added from 100.5 mM stock solutions, and each titration was performed by more than 20 measurements at room temperature. Hexafluorobenzene was used as the internal standard in ¹⁹F NMR studies.

Results and Discussion

L^1 possesses a preorganized tripodal cleft with amide NH protons suitable for anion recognition. Recently, we

have reported the complexation of L^2 with TBA-F, TBA-Cl, TBA-AcO, and TBA-NO₃.^{7b} Among these anion complexes, complexation of L^2 with TBA-F resulted in the discrete dimeric capsular assembly upon encapsulating $[\text{F}_2(\text{H}_2\text{O})_6]^{2-}$ as a guest inside the dimeric capsule, whereas complexes from other anions such as Cl⁻, NO₃⁻, and AcO⁻ do not form the discrete dimeric capsular assembly as observed in the case of fluoride complexation. In the case of L^2 we structurally demonstrated the anionic guest dependent dimeric capsular assembly. When L^1 was treated with an excess of tetrabutylammonium salts of NO₃⁻, AcO⁻, F⁻, and Cl⁻ ions, the complexes $[\text{L}^1 \cdot \text{TBA-NO}_3 \cdot (\text{dioxane})]$ (**1**), $[\text{L}^1 \cdot \text{TBA-OAc} \cdot 4\text{H}_2\text{O}]$ (**2**), $[\text{L}^1 \cdot \text{TBA-F} \cdot 3\text{H}_2\text{O} \cdot 2(\text{dioxane})]$ (**3**), and $[\text{L}^1 \cdot \text{TBA-Cl} \cdot 2\text{H}_2\text{O} \cdot 2(\text{dioxane})]$ (**4**) were isolated in good yield as crystals suitable for single-crystal X-ray studies.

Table 2. Hydrogen-Bonding Interactions in Complexes 1–4

D–H···A	D–H (Å)	H···A (Å)	D···A (Å)	∠D–H···A (deg)
Complex 1 ^a				
N20–H20···O1 ¹	0.76(4)	2.57(4)	3.297(5)	161(4)
N20'–H20'···O7 ¹	0.860(2)	2.175(3)	2.984(3)	156.7(18)
N27–H27···O3 ¹	0.84(4)	2.36(4)	3.181(4)	164(4)
N27'–H27'···O8 ¹	0.860(2)	2.311(2)	3.132(3)	159.79(17)
N43–H43···O3 ¹	0.780(3)	2.34(3)	3.108(3)	169(3)
N43'–H43'···O5 ¹	0.860(2)	2.218(2)	3.040(3)	160.15(16)
C17–H17···O7 ¹	0.929(3)	2.494(2)	3.279(4)	142.39(19)
C34–H34···O5 ¹	0.930(3)	2.569(2)	3.315(4)	137.51(19)
C34'–H34'···O4 ¹	0.931(3)	2.563(2)	3.319(4)	138.58(19)
C50–H50···O8 ¹	0.931(3)	2.591(2)	3.352(4)	139.22(19)
C50'–H50'···O3 ¹	0.930(3)	2.527(2)	3.289(4)	139.32(19)
C51'–H51'···O5 ¹	0.929(3)	2.562(2)	3.451(4)	160.34(19)
Complex 2 ^b				
N15–H15···O1 ¹	0.860	2.050	2.893 (10)	166.18
N22–H22···O72A ²	0.860	2.020	2.836(13)	158.13
N22–H22···O72B ²	0.860	2.491	3.33(2)	165.91
Complex 3 ^c				
N16–H16···O3A ¹	0.88(4)	2.03(4)	2.900(4)	175(3)
N23–H23···O2 ¹	0.80(4)	2.28(4)	3.053(4)	165(4)
N39–H39···F1 ¹	0.86(4)	1.95(4)	2.805(4)	178(3)
C10–H10···O3A ²	0.930(3)	2.327(3)	3.211(4)	158.63(19)
C27–H27···O4B ¹	0.929(3)	2.399(5)	3.325(6)	175.1(2)
Complex 4 ^d				
N5–H5···C11 ¹	0.66(6)	2.65(6)	3.290(7)	166(7)
N21–H21···O50B ¹	0.87(7)	2.36(7)	3.043(13)	136(6)
C25–H25···O50B ¹	0.929(5)	2.509(12)	3.421(13)	167.2(4)
C26–H16···C11 ²	0.930(5)	2.807(2)	3.466(6)	128.8(3)
C45–H45···C11 ¹	0.930(7)	2.708(3)	3.636(7)	176.1(4)

^aSymmetry code: (1) x, y, z . ^bSymmetry codes: (1) x, y, z ; (2) $-x + 2, -y + 1, -z$. ^cSymmetry codes: (1) x, y, z ; (2) $2 - x, 1 - y, 1 - z$. ^dSymmetry codes: (1) x, y, z ; (2) $1 - x, 1 - y, 1 - z$.

Complex 1, [L¹·TBA·NO₃⁻·(dioxane)]. Complex 1 crystallizes in the triclinic system in the $P\bar{1}$ space group along with two dioxane molecules as the solvent of crystallization. The structure of 1 revealed a dimeric capsular assembly of L¹ along with two encapsulated NO₃⁻ ions. Although there is no crystallographically imposed symmetry, the environments around both NO₃⁻ ions are almost identical. The NO₃⁻ guest is in a hydrogen-bonding interaction with the –NH and aryl –CH protons of L¹ (Figure 1a). The oxygen atom O1 of NO₃⁻ (designated by N2) interacts with N20 and N27, whereas O3 interacts with N27 and N43 from above the plane of NO₃⁻, resulting in four N–H···O interactions, with N···O bond distances ranging from 3.11 to 3.33 Å (Figure 1a).

Further, O1, O3, and O4 of the NO₃⁻ are in C–H···O hydrogen-bonding interactions with C16, C50', and C34' with C···O bond distances of 3.53, 3.29, 3.32 Å, respectively, resulting in seven hydrogen-bonding interactions. In case of NO₃⁻ (designated by N6), oxygen atoms O7, O8, and O5 are in three N–H···O interactions with amide protons of N20', N27', and N43', respectively, from below the plane of NO₃⁻ of the other tripodal receptor, with N···O bond distances ranging from 3.0 to 3.1 Å (Figure 1a). Further, O5, O7, and O8 of NO₃⁻ are in three C–H···O interactions with hydrogen atoms of C51' (one interaction with O5) and C35' (two interactions with O7 and O8) of the parent receptor and three more C–H···O interactions with hydrogen atoms of C34,

C17, and C50 of the dimeric partner, resulting in nine hydrogen-bonding interactions. Details of these interactions are mentioned in Table 2. In addition, both of the nitrate ions are in short contact with the respective π cloud of the aryl platform, where the distance between C_g1 (centroid of C22'/C23'/C25'/C39'/C41'/C55') and the nitrogen atom (N6) of the nitrate ion is 3.229 Å and the distance between C_g2 (centroid of C22/C23/C25/C39/C41/C55) and the nitrogen atom (N2) of the nitrate ion is 3.225 Å. The N–H···O interaction observed here can also be regarded as the N–H··· π type, as these interactions are from above/below the plane of NO₃⁻.^{3c} Despite the potential biological relevance of this type of π coordination, the literature contains only a few experimental studies with synthetic receptors.²² Many enzymes preferentially activate their carbon acid substrates through an electrophilic coordination directed toward the π -bond of the carbonyl rather than the conventional lone pair directed model.²³ The CH···O hydrogen-bonding interactions between cleft-bound nitrate and aryl

(22) (a) Snowden, T. S.; Bisson, A. P.; Anslyn, E. V. *J. Am. Chem. Soc.* **1999**, *121*, 6324–6325. (b) Houk, R. J. T.; Monzingo, A.; Anslyn, E. V. *Acc. Chem. Res.* **2008**, *41*, 401–410. (c) Mahoney, J. M.; Stucker, K. A.; Jiang, H.; Carmichael, I.; Brinkmann, N. R.; Beatty, A. M.; Noll, B. C.; Smith, B. D. *J. Am. Chem. Soc.* **2005**, *127*, 2922–2928.

(23) (a) Benning, M. M.; Taylor, K. L.; Liu, R.; Yang, G.; Xiang, H.; Wesenberg, G.; Dunaway-Mariano, D.; Holden, H. M. *Biochemistry* **1996**, *35*, 8103–8109. (b) Vock, P.; Engst, S.; Eder, M.; Ghisla, S. *Biochemistry* **1998**, *37*, 1848–1860.

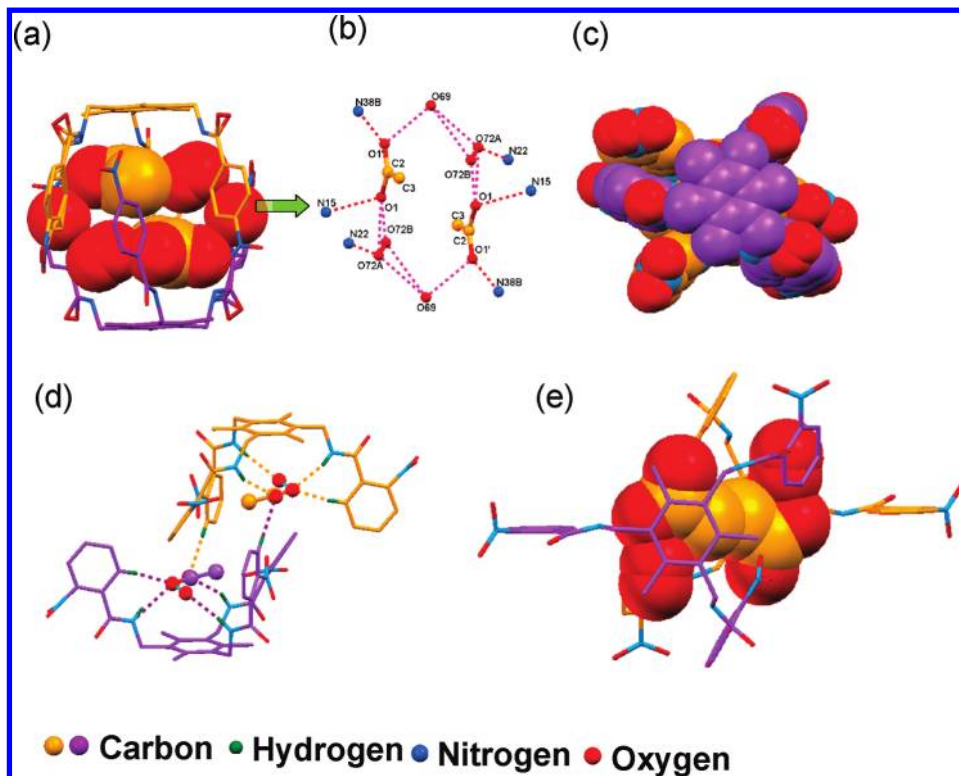


Figure 2. (a) View of the encapsulated acetate ion and water molecules inside the dimeric capsule of **2**. (b) Hydrogen-bonding interactions of acetates and water molecules in **2**. (c) View along the apical benzene cap of the receptor in **2** to show the complete encapsulation of the acetate anions inside the capsule's cavity. (d) Formation of zipperlike assembly of L^2 upon complexation of the acetate ion and water molecule in the tripodal cleft. (e) Apical view to show the encapsulated acetate ions and water molecules in the acetate complex of L^2 . Tetrabutylammonium cations, nonbonding hydrogen atoms, and the lattice solvent molecules have been omitted for clarity.

C–H of other receptor units play a crucial role in bringing the similarly charged anions into close proximity by forming a dimeric capsular assembly. The distance between the central nitrogen atoms of two NO_3^- is 3.562 Å, which is almost comparable with the unusual encapsulation of two nitrate anions reported previously in a protonated polyammonium macrobicyclic receptor.^{2f} The distance between the centroids of apical benzene caps is 10.01 Å, which is greater than the distance observed in the case of an acetate-encapsulated bicyclic cyclophane with a similar head group.^{3c} Though the receptor cavities are the same for L^1 and L^2 , entirely different modes of binding of these receptors with nitrate anion are observed. The nitrate complex of L^2 showed a zipperlike assembly, as shown in Figure 1c,d, which was reported by us in a recent communication.^{7b}

Complex 2, [$L^1 \cdot \text{TBA} \cdot \text{OAc} \cdot 4\text{H}_2\text{O}$]. Complex **2** crystallizes in the triclinic system in the $P\bar{1}$ space group along with four water molecules as the solvent of crystallization. All of the atoms in one of the arms of L^1 in **2** and three water molecules are disordered in two positions. The solid-state crystal structure of **2**, obtained from dioxane, also revealed the dimeric capsular assembly of L^1 with encapsulated hydrated AcO^- . Two AcO^- groups along with four water molecules are encapsulated inside the dimeric capsule (Figure 2a–c).

The anion is encapsulated inside via strong N–H \cdots O and C–H \cdots O interactions with L^1 in addition to the hydrogen-bonding interactions with encapsulated water molecules. The distance between the centroids of the apical benzene caps is 10.245 Å, which is almost similar

to the case in **1**. The encapsulated acetate ions are bridged by the water molecules, and thus these four water molecules overcome the anion–anion repulsion and hold them together inside the dimer. Though both nitrate and acetate ions are geometrically equivalent, their modes of binding vary in the solid state but provide similar dimeric aggregation. In **2**, the encapsulated acetate ion is not hydrogen bonded to the –CH protons of the other receptor of the dimer, as observed in the case of **1**. Instead, the bridging water molecules are involved in hydrogen-bonding interactions to bring other receptors toward the formation of a capsular aggregate (Table 2). In addition, the –CH protons of one encapsulated AcO^- are in a hydrogen-bonding interaction with the other encapsulated AcO^- via C–H \cdots O interactions and hence avoid the anion–anion repulsion inside the dimeric capsule (Figure 2). Comparison of the acetate complex of L^2 with **2** revealed the role of the position of the nitro substituent in the aryl terminal. The acetate complex of L^2 showed the encapsulation of acetate and water molecule inside the tripodal bowl and forms the CH \cdots O interaction assisted zipperlike assembly as observed in the nitrate complex of L^2 (Figure 2d,e).^{7b}

Complex 3, [$L^1 \cdot \text{TBAF} \cdot 3\text{H}_2\text{O} \cdot 2(\text{dioxane})$]. Upon complexation with fluoride in dioxane, the receptor L^1 yielded the complex **3**, which possesses two units of [$L^1 \cdot \text{TBAF} \cdot 3\text{H}_2\text{O} \cdot 2(\text{dioxane})$] in an asymmetric unit. The X-ray crystal structure of **3** revealed the dimeric capsular assembly of the receptor L^1 with encapsulated hydrated fluoride, $[\text{F}_2(\text{H}_2\text{O})_6]^{2-}$, as a guest in the capsule (Figure 3a,b). It is worth mentioning that selective binding of $[\text{F}_2(\text{H}_2\text{O})_6]^{2-}$

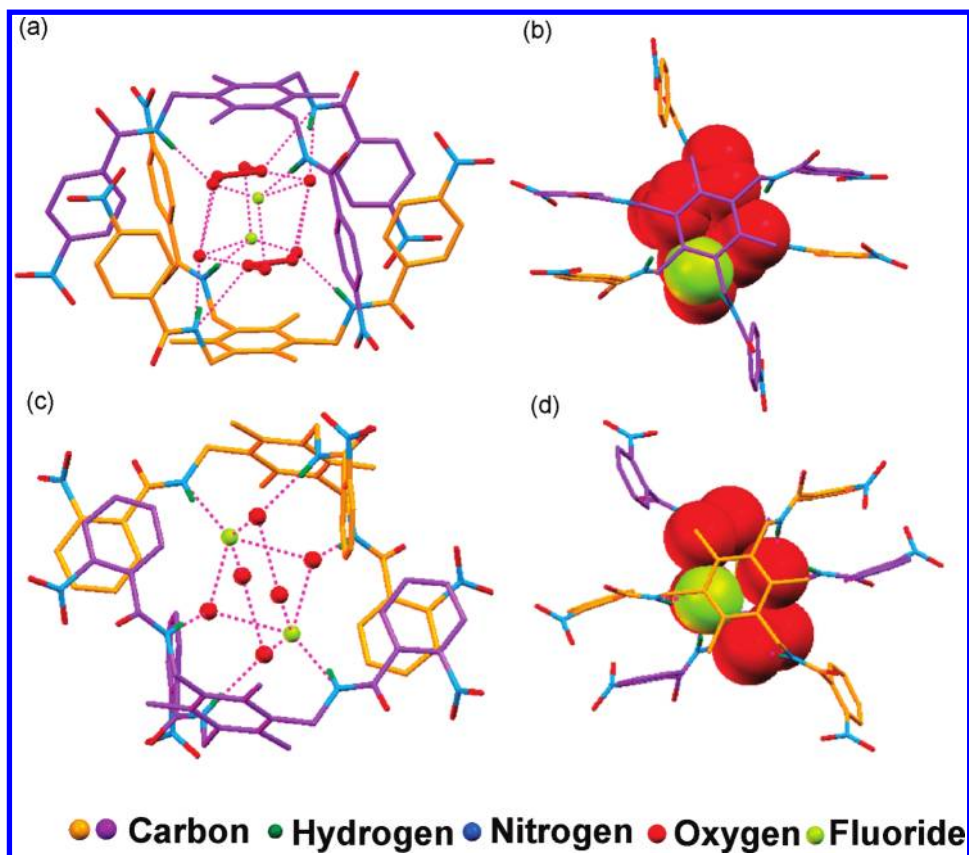


Figure 3. (a) View showing the encapsulated $[\text{F}_2(\text{H}_2\text{O})_6]^{2-}$ cluster inside the dimeric capsule and its interaction with the receptor units in **3**. (b) View along the apical benzene cap to show the cavity encapsulated $[\text{F}_2(\text{H}_2\text{O})_6]^{2-}$ inside the staggered dimeric capsular assembly in **3**. (c) View showing the encapsulated $[\text{F}_2(\text{H}_2\text{O})_6]^{2-}$ cluster inside the dimeric capsule and its interaction with the receptor units in the fluoride complex of L^2 . (d) View along the apical benzene cap to show the cavity encapsulated $[\text{F}_2(\text{H}_2\text{O})_6]^{2-}$ inside the staggered dimeric capsular assembly in the fluoride complex of L^2 . Tetrabutylammonium ions, nonbonding hydrogen atoms, and the lattice solvents are omitted for clarity.

inside the dimeric capsular assembly of L^2 (Figure 3c,d) has been reported recently by us.^{7b} The source of water in the crystal could be from the hydrated TBAF salt and atmospheric moisture. In both the above cases, probably the $[\text{F}_2(\text{H}_2\text{O})_6]^{2-}$ cluster has acted as a template in the formation of the dimeric capsule, where all three arms of the ligand projected in one direction to form a bowl-shaped cavity and two such bowls intercalate to form the dimeric assembly. This template is formed via strong fluoride–water interactions. In **3** four water molecules of the $[\text{F}_2(\text{H}_2\text{O})_6]^{2-}$ cluster are disordered and, in addition to the conventional hydrogen-bonding interactions, fluoride and water molecules of $[\text{F}_2(\text{H}_2\text{O})_6]^{2-}$ are in interactions with aryl C–H protons, resulting in two C–H \cdots F and two C–H \cdots O interactions. Nitro group substitution in the aryl terminals increases the aryl C–H acidity, which facilitates these C–H \cdots F and C–H \cdots O interactions between the two bowls (Table 2). Probably these interactions are the driving force in the formation of a staggered dimeric capsular assembly. All of the encapsulated water molecules are disordered in two positions. Unlike acetate and nitrate complexes, the fluoride complex of L^1 is almost similar to the solid-state structure observed for the fluoride complex of L^2 (Figure 3c,d). In both cases, the cavity encapsulates $[\text{F}_2(\text{H}_2\text{O})_6]^{2-}$ as the anionic guest inside the staggered dimeric capsular assembly (Figure 3b,d).

Complex 4, $[\text{L}^1 \cdot \text{TBA} \cdot \text{Cl} \cdot 2\text{H}_2\text{O} \cdot 2(\text{dioxane})]$. The structure of **4** also revealed a $[\text{Cl}_2(\text{H}_2\text{O})_4]^{2-}$ templated dimeric

capsular assembly of L^1 , though all water molecules are disordered in two positions (Figure 4a–c).

The water–chloride cluster $[\text{Cl}_2(\text{H}_2\text{O})_4]^{2-}$ is in octahedral arrangement formed via strong hydrogen-bonding interactions, as shown in Figure 4b. The binding of another chloride–water cluster, $[\text{Cl}(\text{H}_2\text{O})_4]^-$, in a metal–organic framework is also known in the literature.²⁴ In addition to the hydrogen-bonding interactions with the amide –NH protons, the chlorides and water molecules are in hydrogen-bonding interactions with the aryl –CH protons (Table 2). All these interactions facilitate the formation of a staggered dimeric capsular assembly. When **4** is compared with the chloride complex of L^2 , the receptor L^1 forms the dimeric capsular assembly as it forms with the other anions and L^2 does not form the dimeric capsular aggregate; instead it shows the formation of the distorted noncapsular dimer as shown in Figure 4d,e.

Solution-State Anion Binding Studies. Qualitative ^1H NMR experiments were performed with TBA salts of F^- , Cl^- , AcO^- , and NO_3^- to understand the solution-state behavior of L^1 in the presence of these anions. Disappearance of the amide –NH signal is observed immediately after the addition of TBA-F to the DMSO- d_6 solution of L^1 , whereas a very slight downfield (0.03 ppm)

(24) Custelcean, R.; Gorbunova, M. G. *J. Am. Chem. Soc.* **2005**, *127*, 16362–16363.

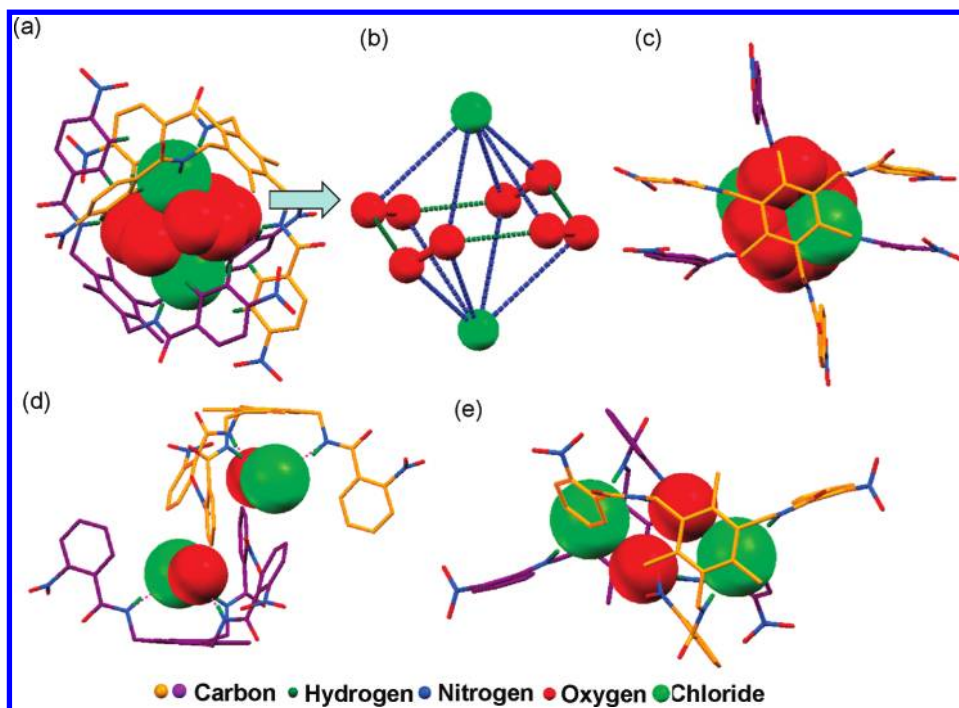


Figure 4. (a) View showing the encapsulated $[\text{Cl}_2(\text{H}_2\text{O})_4]^{2-}$ cluster inside the dimeric capsule in **4**. (b) Hydrogen-bonding interactions of the $[\text{Cl}_2(\text{H}_2\text{O})_4]^{2-}$ cluster. (c) View along the apical benzene cap showing the encapsulation of the $[\text{Cl}_2(\text{H}_2\text{O})_4]^{2-}$ cluster inside the staggered dimeric capsular aggregation in **4**. (d) View showing the encapsulation of chloride–water in the chloride complex of L^2 . (e) View of the chloride complex of L^2 along the benzene cap to show the noncapsular dimeric aggregation. Tetrabutylammonium ions, nonbonding hydrogen atoms, and lattice solvent molecules have been omitted for clarity.

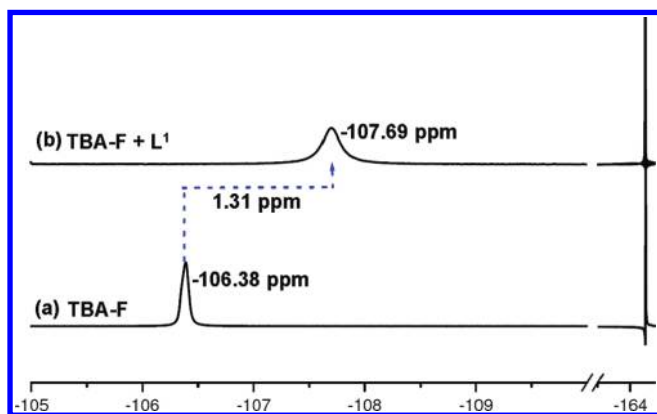


Figure 5. (a) Partial ^{19}F NMR spectrum (500 MHz) of TBA-F in $\text{DMSO}-d_6$ at 298 K. (b) ^{19}F NMR spectrum (500 MHz) of a mixture of L^1 and TBA-F in $\text{DMSO}-d_6$ at 298 K.

shift of the $-\text{NH}$ proton is observed in the case of TBA-Cl and no shift of the $-\text{NH}$ proton is observed in the case of NO_3^- . In the case of TBA-OAc, the chemical shift position of amide $-\text{NH}$ protons shifted 0.2 ppm downfield. In the case of F^- binding studies with L^1 we have carried out ^{19}F NMR in $\text{DMSO}-d_6$ solution (Figure 5). The ^{19}F NMR spectra in $\text{DMSO}-d_6$ revealed that the encapsulation of fluoride anion might persist in solution as well (Figure 5). A free fluoride resonance for *n*-tetrabutylammonium fluoride in $\text{DMSO}-d_6$ appears at 106.38 ppm when hexafluorobenzene is used as an internal standard. The addition of L^1 to the solution of tetrabutylammonium fluoride in $\text{DMSO}-d_6$ results in an upfield shift of 1.3 ppm for the free fluoride resonance, indicating the participation of the anion in hydrogen bonding with $-\text{NH}$ of the receptor L^1 . The diffusion coefficient has

been used as a powerful tool for detecting and probing encapsulation,²⁵ since the encapsulated guests are generally much smaller molecular species than the capsule itself and, therefore, should have a much higher diffusion coefficient in their free state.

The ^1H NMR titration experiments with AcO^- with this receptor showed 1:3 host to guest binding in solution (Figure 6), whereas the solid-state single-crystal X-ray study showed 1:1 binding. Similar solution-state binding was also observed in case of L^2 with AcO^- in $\text{DMSO}-d_6$.^{7b} The difference in binding patterns in the solid and solution states is not uncommon.^{13c} Here, the difference in binding of three acetate anions in solution versus one acetate in the solid state may be due to multiple equilibria or side cleft binding of anions in the solution state, which could allow multiple anion interactions with a single receptor. Further, solvent systems (dioxane vs dimethyl sulfoxide) might have played an important role in imposing different binding patterns observed in the solid and solution states. To probe the highest selectivity of L^1 toward F^- over Cl^- , NO_3^- , and AcO^- , we carried out a series of qualitative ^1H NMR experiments in the presence of various anions or mixtures of anions (Figure 7). In case of the spectrum shown in Figure 7b, the experiment was carried out upon addition of excess TBA- NO_3 to a solution of L^1 in $\text{DMSO}-d_6$. No appreciable change in chemical shift was observed upon addition of NO_3^- to L^1 . When chloride salt was added to the L^1 solution in the presence of nitrate, a very slight (0.1 ppm) change in chemical shift was observed (Figure 7c), and when excess

(25) Cohen, Y.; Avram, L.; Frish, L. *Angew. Chem., Int. Ed.* **2005**, *44*, 520–554. In our cases, a distinct NMR signal is not observed for the encapsulated water molecules and the bulk water and hence we could not perform DOSY experiments for probing the encapsulated water inside the capsules.

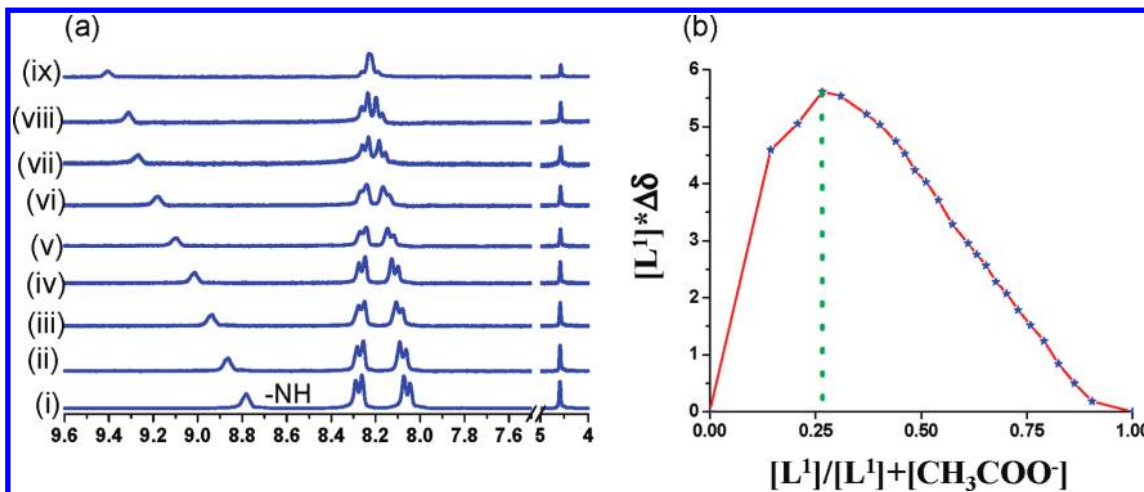


Figure 6. (a) ^1H NMR (300 MHz) spectral changes of L^1 with added TBA- AcO^- in $\text{DMSO-}d_6$ (25 $^\circ\text{C}$) ($[\text{H}]_0 = 16.2$ mM). Ratio of concentration $[\text{G}]/[\text{H}]$: (i) 0; (ii) 0.27; (iii) 0.48; (iv) 0.74; (v) 1.06; (vi) 1.49; (vii) 2.23; (viii) 2.76; (ix) 6.37. (b) Jobs plot for the binding of acetate anion to the host L^1 .

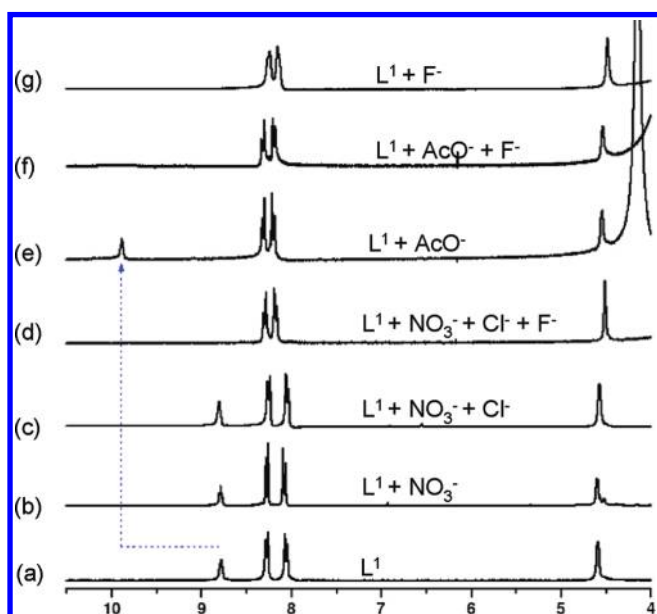


Figure 7. Partial ^1H NMR spectra (300 MHz, $\text{DMSO-}d_6$, 298 K) of L^1 (a) and spectral changes upon addition of various anions or mixture of anions as their tetrabutylammonium salts, as noted in the individual spectra (b–g).

F^- was added to this mixture containing NO_3^- and Cl^- with L^1 , the $-\text{NH}$ protons of the amide signals disappeared in addition to appreciable changes in the aryl $-\text{CH}$ protons (Figure 7d). Upon charging an excess of AcO^- salt to L^1 , we observed a huge change in chemical shift positions of amide $-\text{NH}$ protons as well as appreciable shifts in the aryl $-\text{CH}$ protons (Figure 7e). When F^- was added to the solution containing L^1 and AcO^- , the amide protons of L^1 disappeared along with changes in the chemical shift positions of aryl $-\text{CH}$ protons. These observations indeed prove the selectivity of the receptor toward the binding of F^- over Cl^- , NO_3^- , and AcO^- . We have also performed crystallizations from mixtures of anions to probe the selectivity in the solid state as well.

Crystals suitable for single-crystal X-ray structural analysis are also isolated when a dioxane solution of L^1 is allowed to complex with 3 equiv each of TBA salts of NO_3^- , AcO^- , F^- , and Cl^- at room temperature for a few days. The structural studies confirmed formation of complex **3** from the mixtures. These studies showed selectivity toward the formation of a $[\text{F}_2(\text{H}_2\text{O})_6]^{2-}$ encapsulated dimeric assembly by L^1 .

Conclusions

In conclusion, L^1 , a positional isomer of L^2 , could encapsulate hydrated acetates, hydrated chlorides, and nitrates in addition to hydrated fluorides in capsular forms. Upon simple alteration of $-\text{NO}_2$ group substitution from the ortho to the para position in the receptor design, a marked difference in aggregational properties is observed in the presence of an anionic guest as well as hydrated anionic clusters that established L^1 as a versatile system for encapsulation of anions in the dimeric capsular assembly. The solid-state demonstration of anion or hydrated anionic guests by this versatile receptor could be useful in alkali-metal salt separation technology. Further, the hydrated fluoride selectivity of this receptor has potential application toward the selective removal of fluoride in its hydrated form. Presently we are exploring similar receptors for such applications.

Acknowledgment. P.G. gratefully acknowledges the Department of Science and Technology (DST), New Delhi, India, for financial support. M.A. acknowledges the CSIR, New Delhi, India, for a Senior Research Fellowship. X-ray crystallography studies were performed at the DST-funded National Single Crystal X-ray Diffraction Facility at the Department of Inorganic Chemistry, IACS.

Supporting Information Available: Figures giving ^1H NMR, ^{13}C NMR, and HRMS (ESI) spectra and CIF files giving crystallographic data for complexes **1–4**. This material is available free of charge via the Internet at <http://pubs.acs.org>.